5

Tunable Rare-Earth Doped Fiber Laser

Arturo A. Castillo-Guzman and Romeo Selvas-Aguilar
Physical and Mathematical Sciences Research Center (CICFIM) UANL-FCFM
San Nicolás de los Garza, Nuevo León,
México

1. Introduction

Recently, researches worldwide have been focused in building up systems capable to increase the output optical powers as well as to improve the beam quality of the delivering system of fiber lasers. Notwithstanding, the demanding of sources in the telecom industry together with the increasing in required bandwidth, need sources with multi-wavelength emissions or tunable sources. The main advantage of tunable sources is due to the fact that by using a single source is possible to tune a laser gain medium at different wavelengths. For example, this feature allows having high quality sources for the telecom application.
Many techniques have been then developed in order to obtain a wide tuning range. Using bulk grating (Chen et al., 2003), fiber Bragg grating (Xia et al., 2006; Goh et al., 2003; Mokhtar et al., 2003), SOA fiber laser based on Sagnac loop mirror via polarization tuning (Zhang et al., 2009), and Fabry-Perot cavity (Chawki et al., 1993) are some example of them. However these techniques are relative expensive or might required very sophisticated setups.
Recently, the multimode interference (MMI) effect has demonstrated to be applied in a wide variety of applications. Because of its wavelength dependence, it works as a wider band-pass filter which is therefore well useful to our tuning mechanism.
On the first part of the chapter, it is analyzed the basic feature of the MMI effect as well as the research carried out by applying this idea in tunable fiber laser systems. These two aspects are well detailed reviewed and subsequently established as the bases for an application of a high power tunable rare-earth optical fiber laser. Parameters like total tunable range, signal to noise ratio, laser line-width are presented.
The second part describes an erbium-doped fiber optical amplifier numerical simulation in a MOPA configuration with a seed signal obtained from a tunable erbium-doped fiber laser (EDFL) based on the MMI effect. The MOPA amplifier was designed using a double-cladding erbium-doped fiber (DC EDF), pumped with a 10 Watts high-power 980nm diode laser. Based on the MMI effect, the tunable filter source of the tunable EDFL is composed by a no-core optical fiber and a ferrule of 127 microns of diameter in a ring laser cavity. The tunable range achieved was 24 nm. This tunablility is from 1576-1600nm which corresponds to the C and L band of the telecomm. The output power was roughly 2.7 Watts with a line-width of 0.1nm. This setup demonstrates to be a portable, no expensive optical fiber laser.

2. Multimode interference effect

The self-imaging feature of a homogeneous multimode planar optical waveguide has been applied in the design of passive planar monomodal optical couplers based on multimode

interference (MMI) (Soldano et al., 1992). This characteristic is described as an input field profile which is reproduced in single or multimode images by mode interference at periodic intervals along the propagation direction of the guide. The self-imaging was firstly suggested by (Bryhgdahl, 1973) and by (Ulrich, 1975a, 1975b).
On one hand, the theory of multimode interference has been also introduced by (Bachmann et al., 1994, 1995) and (Soldano & Pennings, 1995). A high performance multimode interference filter was also proposed by (Li et al., 2002) for 1.3 and 1.5μm regions. These works do not described the self-imaging for optical fibers. On the other hand and using this effect a wavelength tuning fiber laser was reported by (Selvas et al., 2005). Later on, an enhancement of this work was reported by increasing the tunable range from 8nm to 12nm (Anzueto-Sanchez et al., 2006).
Taking into account Fig. 1 which is a schematic diagram of the minimum length required to this effect takes place, the mathematical expressions behind this effect are as followed.

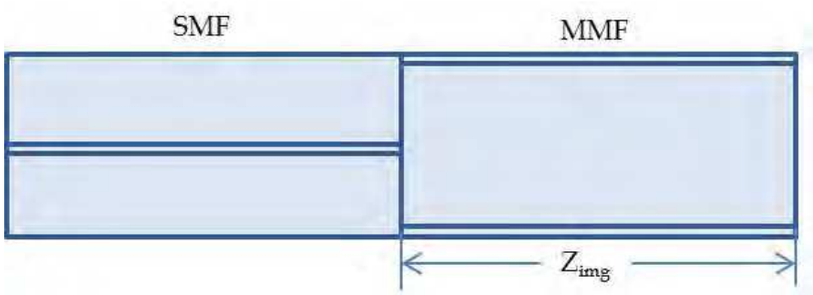

Fig. 1. A schematic diagram in which the multimode interference effect takes place in optical fibers.

The field distribution at the end of the MMF segment of length z, can be written as (Mohammed et al., 2004)

$$E_{MMF}(r,\theta)=\sum_{j=0}^{M} a_j \psi_j(r,\theta)\exp\left(i\beta_j z\right), \tag{1}$$

where ψ_j and a_j are the jth mode electric field amplitude and the field expansion coefficient, respectively. The constant M is the total number of guided modes inside the MMF. For on-axis coupling, the number of modes is reduced to the number of radially symmetric modes. The field expansion coefficients in Eq. (1) can be calculated from the following cross-correlation formula:

$$\alpha_j=\frac{\int_{\theta=0}^{2\pi}\int_{r=0}^{\infty} E_s(r,\theta)\times\psi_j(r,0)^* \, r dr d\theta}{P_j},$$

$$P_j=\int_{\theta=0}^{2\pi}\int_{r=0}^{\infty}\left|\psi_j(r,\theta)\right|^2 r dr d\theta. \tag{2}$$

In Eq. (2), E_s is the field distribution of the SMF fundamental mode. The power coupling efficiency to the second SMF is calculated through the overlap integral between E_{MMF} and the second SMF fundamental mode.

Now, considering the single reimaging of the input field, it occurs at specific longitudinal locations within the MMF where $|\psi(r,z)|=|\psi(r,0|$. This occurs at periodic longitudinal z locations (Mehta et al., 2003)

$$z_{img}(\lambda)=\frac{\frac{m\pi}{2}}{\beta_{inside,0}(\lambda)-\beta_{inside,1}(\lambda)}, \quad m=1,2,3,... \tag{3}$$

where $\beta_{\text{inside},0}$ and $\beta_{\text{inside},1}$ represent the longitudinal propagation constants within the MMF. These terms are determined using the weakly guiding approximation and applying physical dimensions and material properties of the MMF into the dispersion relations that characterize propagation within the optical fiber.

Continuing with the analysis of this effect, the reimage that comes out of the MMF has been used in order to get an optical device (Soldano et al., 1992; Li et al., 2002; Selvas et al., 2005; Anzueto-Sanchez et al., 2006; Mehta et al., 2003). All these works used a high reflector mirror to get the light back into the MMF again as is showed in Fig 2. The analysis goes further because of the free space condition. Eq. (4) gives the relation between the mirror distance expression and the maximum coupling of light back into the SMF (Mohammed et al., 2004)

$$z_{out}(\lambda)=\frac{\frac{\pi}{2}-\left\{\left(L_{MMF}\right)\left(\beta_{inside,0}(\lambda)-\beta_{inside,1}(\lambda)\right)\right\}}{\beta_{out,0}(\lambda)-\beta_{out,1}(\lambda)} \tag{4}$$

where L_{MMF} is the length of the multimode optical fiber.

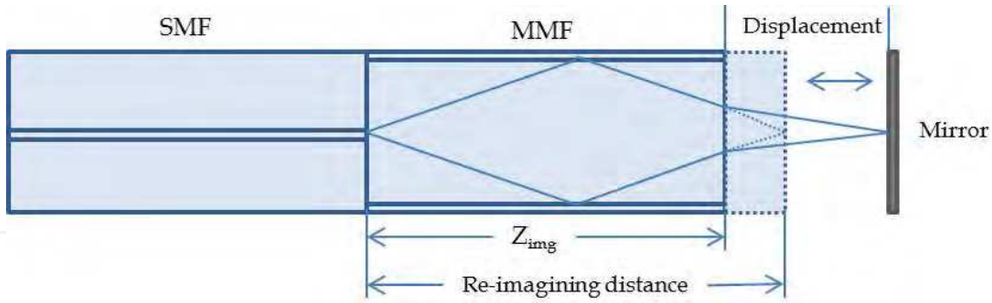

Fig. 2. SMF/MMF/mirror in free space setup.

In other words, the length at which single images are formed can be obtained from the restricted symmetric interference condition which is given by (Selvas et al., 2005 or Mehta et al., 2003)

$$L=p\left(\frac{3L_{\pi}}{4}\right) \quad \text{with p = 0,1,2,…,} \tag{5}$$

where L_{π} is the beat length

$$L_{\pi}\cong\frac{4n_{MMF}W_{MMF}^{2}}{3\lambda_{0}}. \tag{6}$$

where n_{MMF} and W_{MMF} correspond respectively to the refractive index and diameter of the MMF core, with λ_0 as the free space wavelength.
Once established the basic principle and the mathematical equations of the MMI effect, in the next section, it will present three different tunable optical fiber lasers in which their tunable systems are based on the MMF theory, and each of them have modified aspects of the MMI effect in order to improve the optical results.

3. Tunable optical doped fiber laser based on MMI effect

Recently, the multimode interference effect has showed so much interest to build up different optical device. A lot of groups all around the world have introduced this effect into their own research. The multimode interference effect has been applied on several optical devices, especially in optical fiber based source, such as: multi-wavelength fiber laser (Poustie et al., 1994), all-fiber refractometer sensor (Wang & Farrell, 2006), high-temperature sensor (Li et al,. 2005) and wavelength tunable laser (Selvas et al., 2005). The latter research area is mainly the focused of this chapter.

3.1 Tunable double-clad ytterbium-doped fiber (DCYDF)

This laser consists of a double-clad ytterbium-doped fiber (DCYDF) with 6/125 μm of core/cladding diameter and an 0.14/0.45 numerical apertures (Martinez-Rios et al., 2003). The length of the DCYDF was 16 m, which corresponds to 7.2 dB of pump absorption (just the 80% of the pump is absorbed). The setup employed is depicted in Fig. 3.

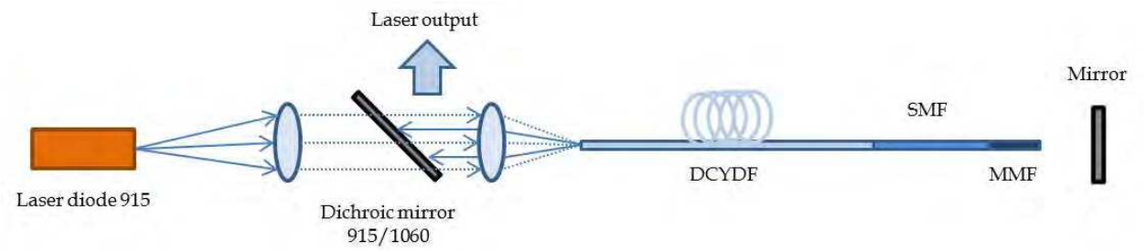

Fig. 3. Set up of the tunable double-clad ytterbium-doped fiber laser.

This tunable laser consists in a laser diode at 915 nm and 5 watts as output power. The light was launched into the DCYDF by two lenses which were AR coated. The DCYDF was fusion spliced to the MMI filter (SMF and MMF), after that, it was set a mirror in order to get the light feedback into the MMF. It was also added a dichroic mirror in order to obtain the output laser power as well as protection to the laser diode.
It is reported by the authors that the broadband mirror was placed at this position, and wavelength tuning was then demonstrated by varying the distance between the broadband mirror and the output facet of the MMF. The separation distance between the mirror and the MMF were achieved by steps of 25 micros where the output power and the optical spectrum of the tunable laser were measured. Fig. 4 shows the relation between the separation distance in steps of the MMF from the mirror and the wavelength tuned.
It can be notice from the Fig. 4. that the linearity tendency are coming from the steps moving away the MMF and the mirror in relation with the wavelength range tuned. It is also demonstrated that the total tuning range was only 8 nm (1088nm to 1097nm). The measured

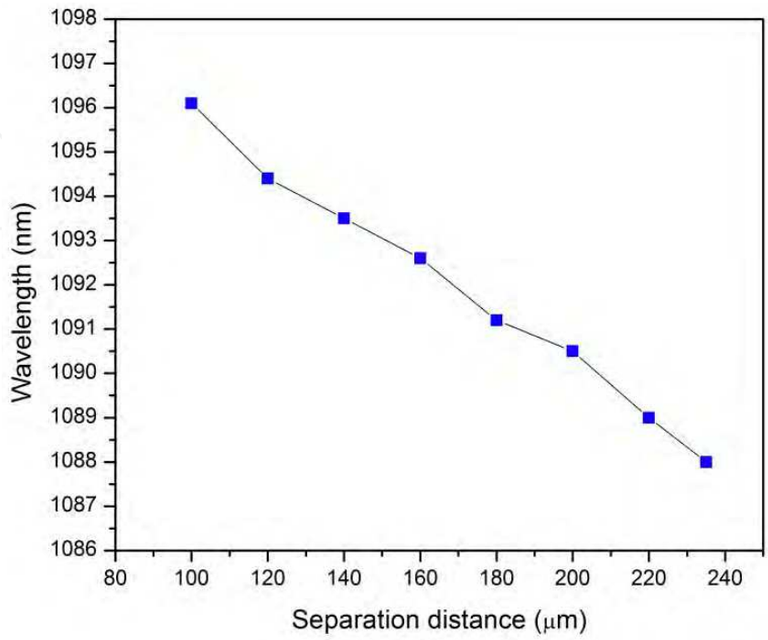

Fig. 4. Tuning wavelength range of the YDFL vs. separation distance of the mirror.

line-width was roughly 0.5 nm and the signal-to-noise ratio better than 30 dB. This optical spectrum is showed in Fig.5.

Additionally, it is reported that an average of 500 mW was obtained with the minimum and maximum power being 460 and 550 mW, respectively. For separation distances shorter than 100 microns and longer than 250 microns, the lasing emission vanished and it is notice that does not correlate to the emission cross section spectrum of the Yb ions. If the goal is to extend the tuning range, it is needed to use a mirror with a flat spectral response within the Yb-gain spectra, and consequently to take advantage of the whole gain range of the ytterbium-doped fibers. The reflectivity of the mirror at 1100-1320nm is about 95% and this reflectivity drops drastically to about 73% from 1100-1070 nm. It is also mentioned that the alignment process have been converted in a tedious work.

3.2 Enhanced tuning mechanism in fiber laser based on multimode interference effect

Taking into account the problems faced on the previous work, a new proposal was then analyzed. Now, an enhanced design for a tuning mechanism was developed (Anzueto-Sanchez et al., 2006). In this occasion, an SU-8 fiber gripper structure was fabricated. This device would align much easier the MMF along with a gold-coated fiber (golden facet) as a fiber mirror. It was also implemented a micrometric stepping motor which was attached to the gold-coated fiber to control the separation distance between the two fibers. Fig. 6. shows the experimental set up of this tunable optical fiber laser.

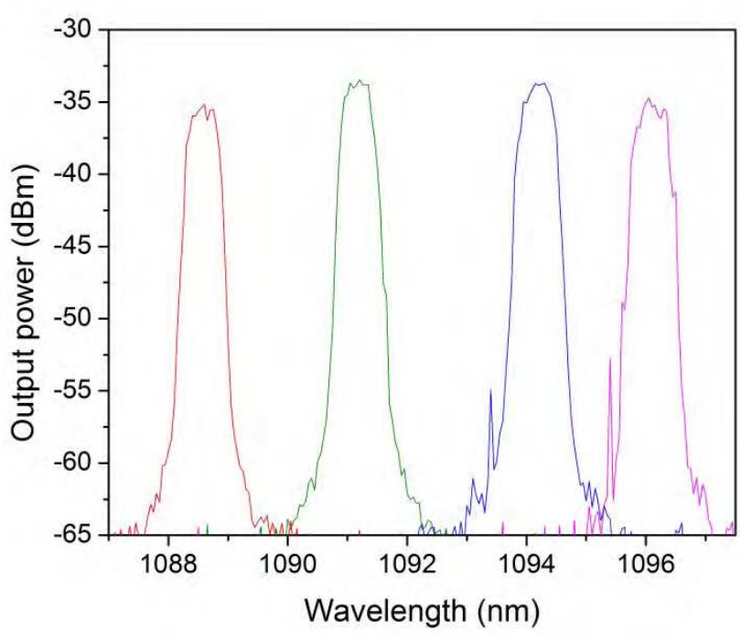

Fig. 5. Total optical tuning range of a DCYFL.

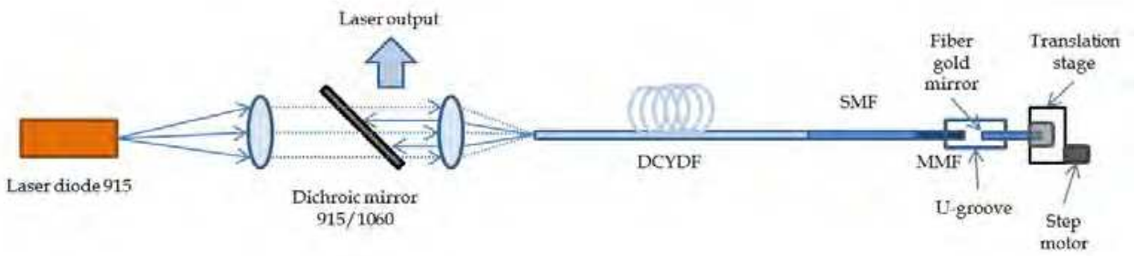

Fig. 6. Schematic diagram of the experimental setup.

The experimental setup was design similarly to the previous one. The important difference lay out in the tunable mechanism. The DCYDF is pumped by a fiber pigtailed multimode laser diode launching the light through two aspheric lenses to one end of the Ytterbium fiber with a maximum power of 1.8 W at 915 nm. To separate the pumping wavelength and the laser emission, it was set a dichroic mirror. The other end of the Ytterbium fiber was fusion spliced to the filter. Fig. 7 shows the tuning device proposed.

The tuning device consists of a SU-8 fiber gripper which is a channel with negative slope walls. The structure was able to grip both fibers once these were inserted in the groove, let them moving along their longitudinal direction giving them an automatic x-y alignment. The fabrication process of the SU-8 structures is well explained in (Raymond et al., 2004). In this case, one fiber is the MMF while the other is the mirror-fiber. It was used a standard thermal evaporator in order to coating a gold film on one facet of a single mode fiber. The MMF was fixed to the SU-8 and the fiber mirror was attached to a computer controlled micrometric stepping motor getting a better displacement control of the fiber, as is showed in Fig. 6.

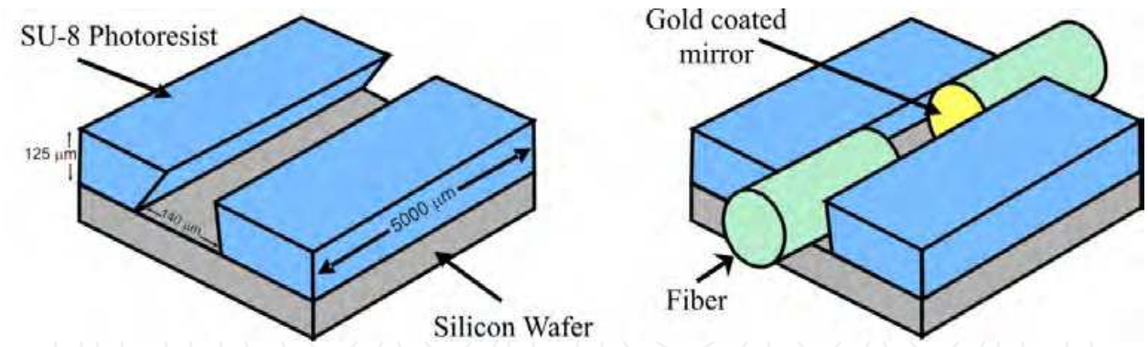

Fig. 7. Wavelength tuning SU-8 device.

Fig. 8. Shows the relation between the separation distance between the MMF and the mirror.

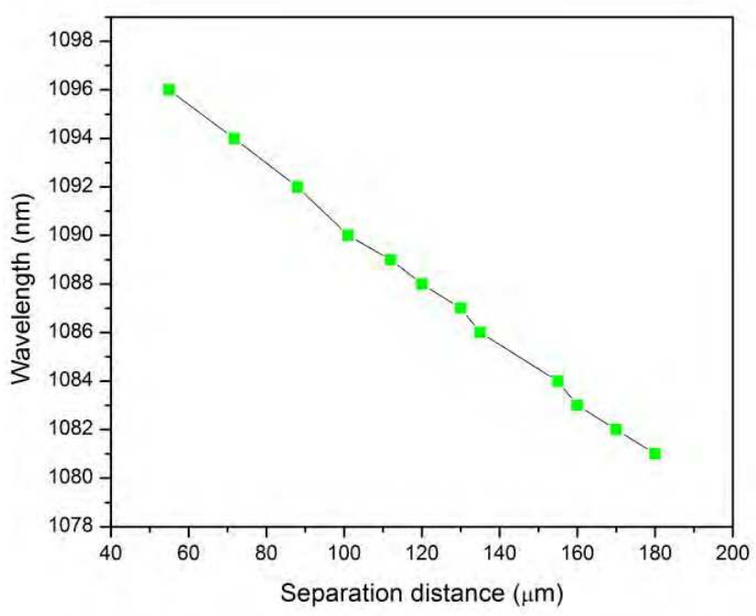

Fig. 8. Experimental results of displacement of facet mirror fiber versus emitted laser wavelength.

It is understood from Fig. 8 that a quasi-linear wavelength tuning against the separation between the MMF and the fiber mirror is obtained. A total tunable range of 12.24 nm was measured and the slope efficiency was around 30% at each wavelength.
The alignment problems were reduced considerably; and an improvement in the total tunable range was therefore achieved, increasing it from 8 nm to 12.24 nm when comparing it with the last section work.

3.3 Tunable multimode interference filter

The maximum tuning wavelength range achieved with the previous set up has been limited to only 12 nm. This limitation is not due to the MMI filter itself, but rather from other effects arising from the way of its implementation. Considering that the peak wavelength response of the filter exhibits a linear dependence when the length of the MMF is modified, a

capillary tube was filled with a refractive index matching liquid as a new proposal. This implementation was figure out in order to increase the length of the MMF as well as the total tuning range (Antonio-Lopez et al., 2010). From the equations (5) and (6) it is possible to obtain an expression in terms of other parameter, the emission wavelength,

$$\lambda_0 = p\left(\frac{n_{MMF}D_{MMF}^2}{L}\right) \quad \text{with p = 0,1,2,…..} \tag{7}$$

This equation is indicating us that if we want to tune in wavelength, the parameters to modify are: the refractive index, the length of the MMF, or the diameter of the MMF. This work proposed the modification of the MMF length as a first option. It was then used a fused silica (n=1.444) ferrule with an inner diameter of 127 μm, and an outer diameter of 5 mm. The process consists in fill the ferrule with a high refractive index liquid with n=1.62 (Cargille Index Matching Liquid), so a liquid multimode waveguide (MMW) would take place inside of the ferrule. As it is explained in[14], the SMF and MMF were inserted in the ferrule, then, at every step the two fibers were moving apart to each other, the space created between them would fill with the refractive index liquid; so the effective length of the MMF will be the sum of the real MMF length plus the liquid MMW segment. As a consequence, if the effective length of the MMF is increased, the wavelength response should be tuned. The set up used is showed in Fig. 9. An important factor was the MMF used. It is also demonstrated that having a bigger refractive index difference between core and cladding provides a MMI filter with narrower linewidth and better contrast (Mohammed et al., 2006). The MMF used is known as no-core, which it is a 125 μm of diameter with air as the cladding.

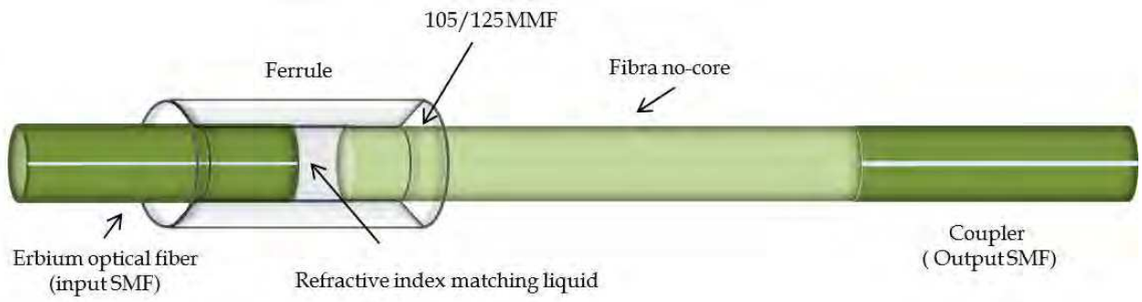

Fig. 9. Schematic of the tuning mechanism with a liquid MMW segment.

There was a deep study in order to obtain the best multimode fiber for the filter. The finite Difference Beam Propagation Method (FD-BPM) was used to numerically model the MMI effect that occurs in the MMF. All the fibers considered for the simulations were those which are commercial. Considering Eq. (5) the autoimages must be formed periodically along the MMF. Nevertheless, due to the nature of the MMI effect, the real output field images are given each 4th image. Fig. 10 to Fig. 13 shows these simulations.

Fig. 10 to Fig. 13 were obtained from a simulation on the BeamPro program. The parameters used in Fig. 13 were the no-core´s. This multimode fiber shows to be the better option for the filter due to its own optical properties along with the possibility to do the filter in the practice. As can be seen in Fig. 13 there are different reimages with different intensities, these formed images at several distances are known as pseudoimages. Most of them are

similar to the input field but they show some losses, therefore, the filter operates with the 4th image.

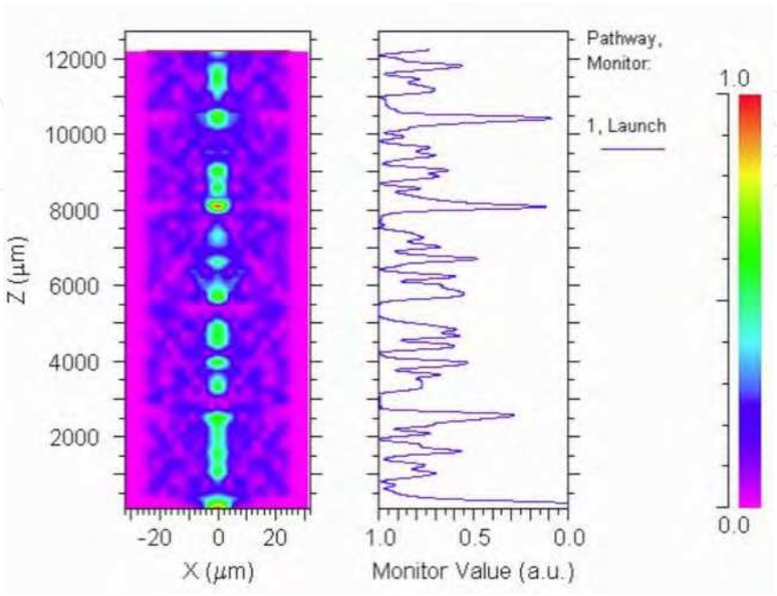

Fig. 10. Beam propagation of a 50/125 μm MMF for 1575 nm.

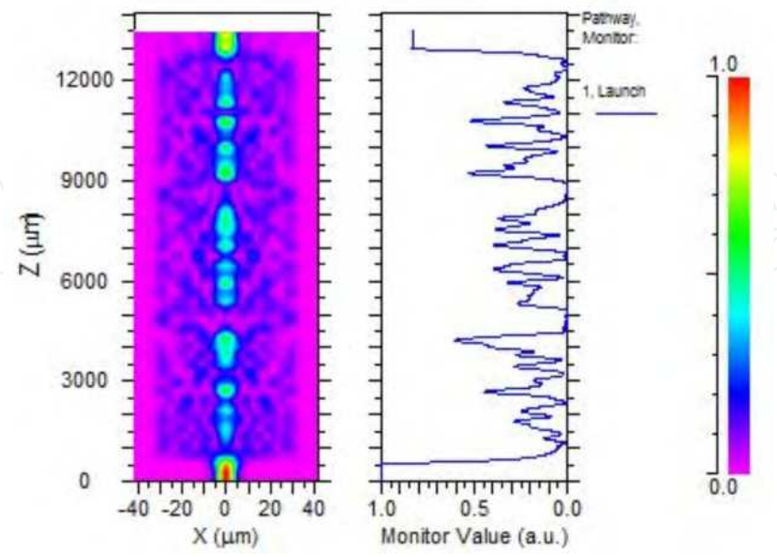

Fig. 11. Beam propagation of a 62.5/125 μm MMF for 1575 nm.

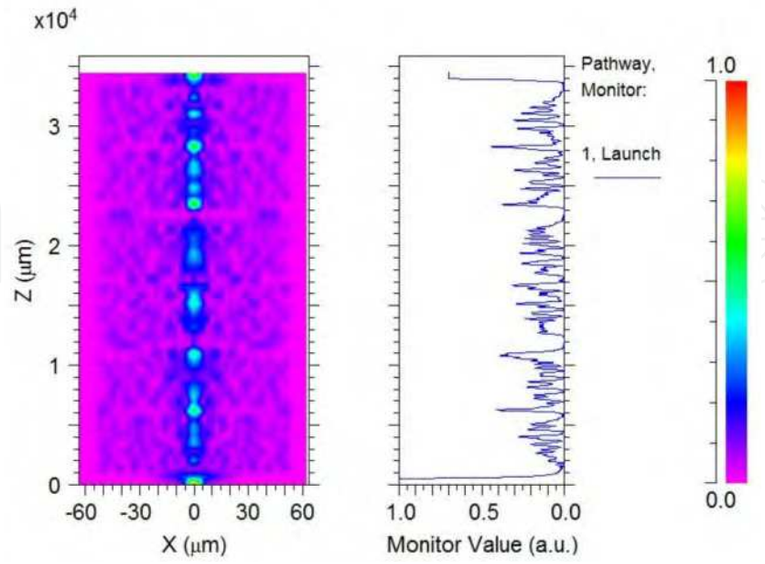

Fig. 12. Beam propagation characteristics of a 105/125 μm MMF for 1575 nm.

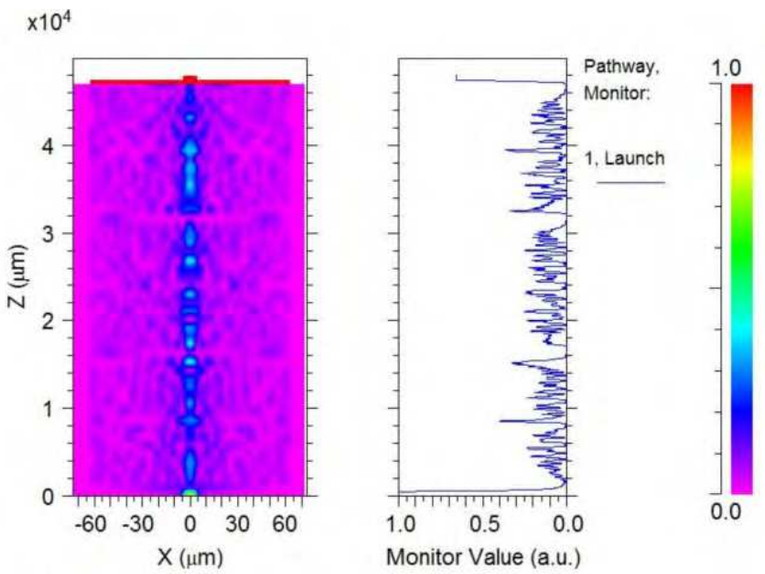

Fig. 13. Beam propagation characteristics of a 125/125 μm MMF for 1575 nm.

Now, since it was used a refractive index liquid which trends to accumulate in the end of the ferrule, it was decided to split the numbers of images in two different multimode fibers. The first re-image was obtained on the 105/125 MMF, the next third re-images were obtained on the no-core fiber. The length of both fibers would be calculated from Eq. (7). By this way, losses due to the contact of the liquid refractive index with the no-core fiber were avoided.

This tunable multimode interference bandpass filter is added to an erbium doped fiber ring-laser. The set up used is showed in Fig. 14.

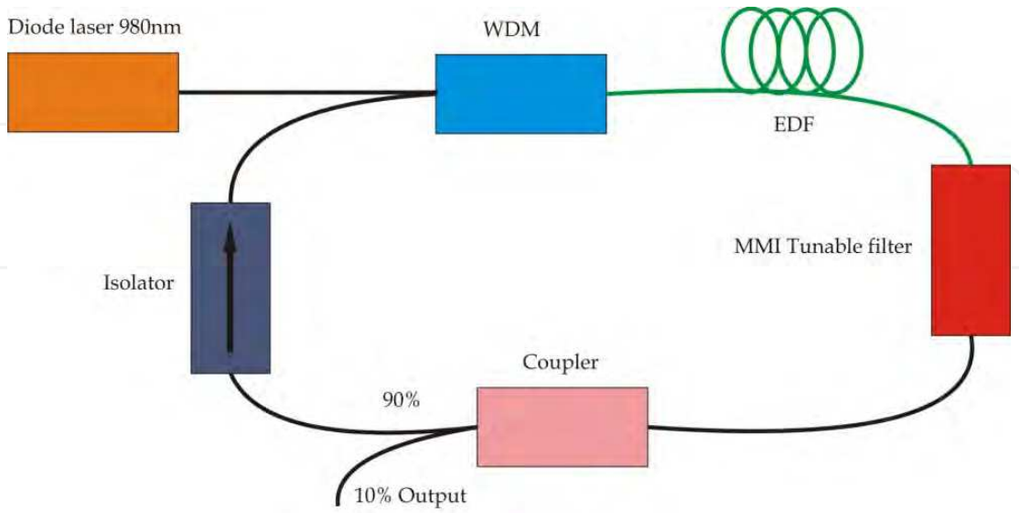

Fig. 14. Schematic set up of a tunable erbium doped fiber laser based on MMI effect.

The experimental set up consists on a laser diode at 980 nm with an output power of 150 mW, a WDM coupler of 980 nm/1550 nm, 5 meters long of Erbium doped fiber (EDF), a C-band optical isolator to keep the laser unidirectional , a 10/90 coupler to monitor the tunability of the laser, and the MMI tunable filter.
Fig. 15 shows the relation between the separation distance between the SMF and the 105/125 MMF. The response of the filter was at every 200 μm.

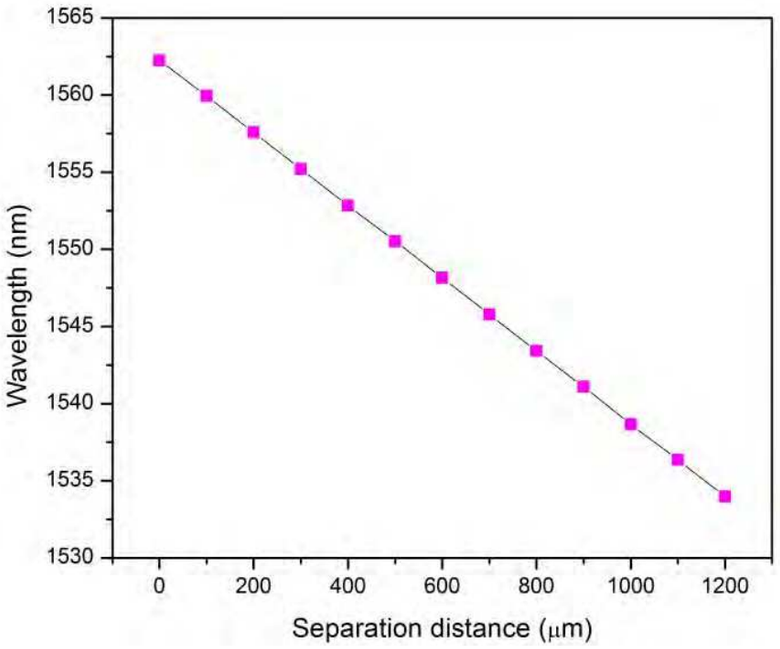

Fig. 15. Wavelength versus separation distance between SMF and 105/125 MMF.

Finally with the implementation of a liquid index matching fluid (n=1.64) inside of a ferrule a tuning range of almost 30 nm was achieved with an insertion losses of 0.4 dB with a 3 dB bandwidth of 0.35 nm as it is showed in Fig. 16.

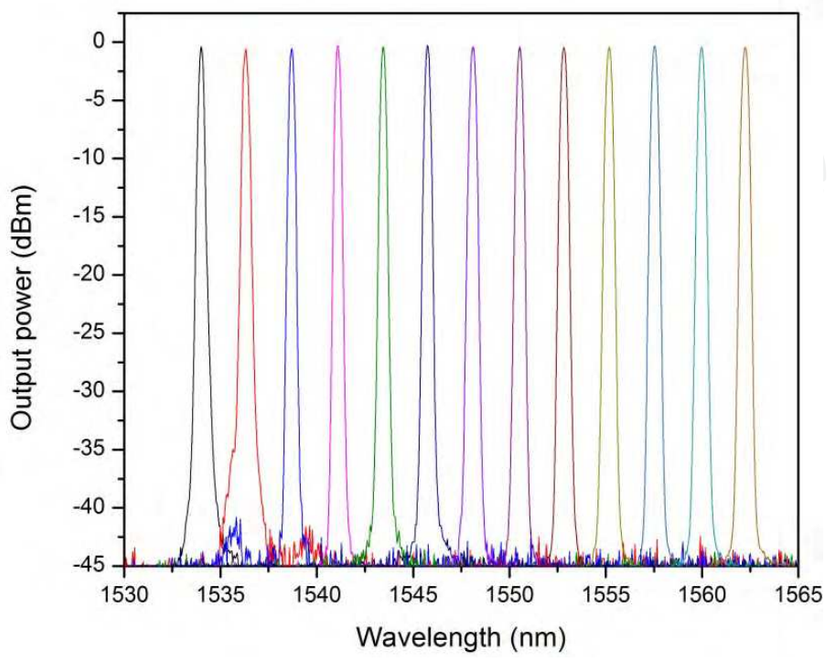

Fig. 16. Wavelength versus Output power with a multimode interference filter.

3.4 A liquid multimode waveguide segment means more tunable range

After the work done so far with the implementation of a liquid index matching liquid (n=1.64), several questions were on the table, for example, how far can be gone with the tunable range?, depending on what?. So, on a try for answering these questions, the spectral response of a group of liquid index matching fluids were studied (Castillo-Guzman et al., 2010). Taking into account that as it is demonstrated in Eq. (7), the peak wavelength response of the MMI filter can be selected by simply changing the length of the MMF, and it was necessary to design a mechanism to change the length of the MMI in real time, creating a liquid waveguide. Previously, it was analysed a liquid index matching fluid of 1.64 as refractive index. Now, the proposal was a deep study of several index matching fluids in order to enlarge the waveguide which gives a larger tunable range as a consequence. Fig. 17 shows the relation between the refractive index of the index matching fluids versus the FWHM.

The index matching liquids were provided by Cargille Labs. It is important to remember that the refractive index of the liquid has to be higher than that of the ferrule and lower than the no-core fiber in order to prevent losses. Fig. 17 shows that the bandwidth increases along with the refractive index. Therefore, since the ferrule refractive index is 1.444 and the no-core fiber is 1.463, it was selected the 1.45. Another change done in this work was that the MMF length was design using only no-core fiber instead of two different MMF.

The set up used was similarly of the Fig. 9, with the exceptions of the variations of the index matching fluids and the use of the no-core fiber as the unique MMF. Fig. 18 shows the set up

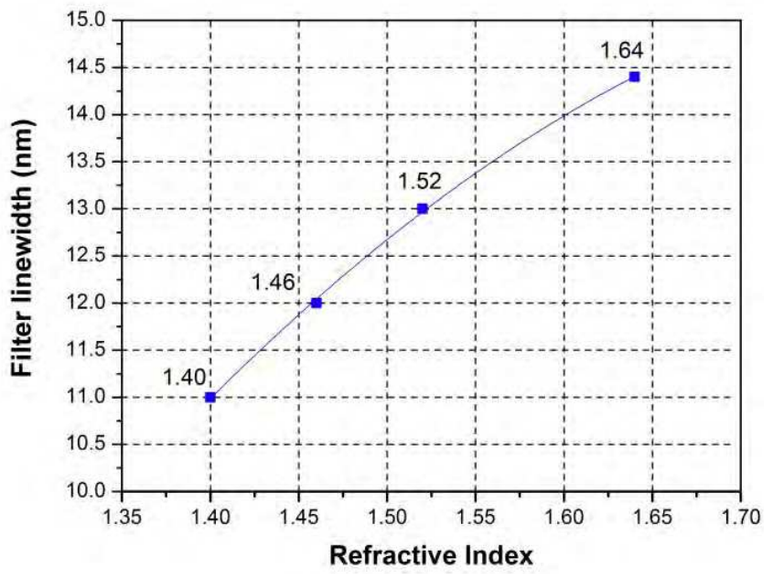

Fig. 17. Refractive index of different index matching fluids vs. MMI filters bandwidth at FWHM.

used in this occasion. About of the elements used in the set up, it was reported a L-band Erbium-doped fiber (EDF) with 2.85 m long, 0.25 NA and 3000 ppm of Er-concentration. A 980 nm laser diode with 150 mW of maximum output power from Lucent Technologies as the pump source. The rest of the elements remained the same.

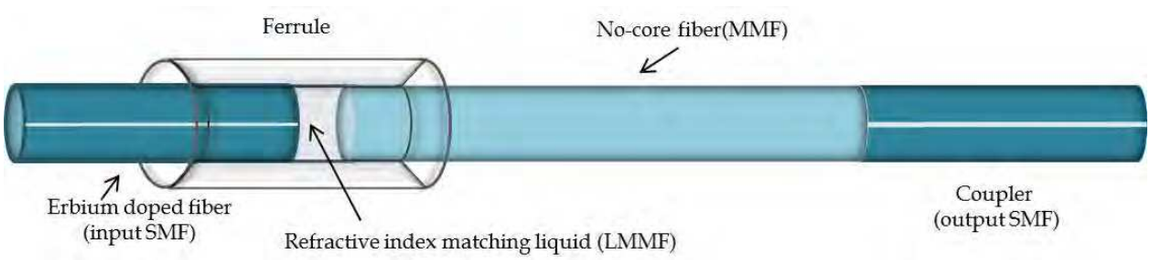

Fig. 18. Set up of a tunable erbium doped fiber laser with a liquid waveguide as a filter.

In order to obtain a tunable range, the EDF and the no-core fiber were separated. The first results obtained are shown in Fig. 19. Here, is shown the relation between the separation distance and the wavelength tuned. The wavelength tuning was achieved varying this separation in 50 μm steps, within a total of 1.6 mm. The index matching fluid used was the 1.64.

The total tuning range was of 39nm. It was from 1561.98nm to 1600.76nm. The linewidth measured was of 0.4nm and the signal to noise ratio was of 40dBm. These experimental results are showed in Fig. 20. The MMI filter has proved to be confident for an erbium optical fiber laser. The tuning mechanism was applied back and forth maintaining the output power always stable.

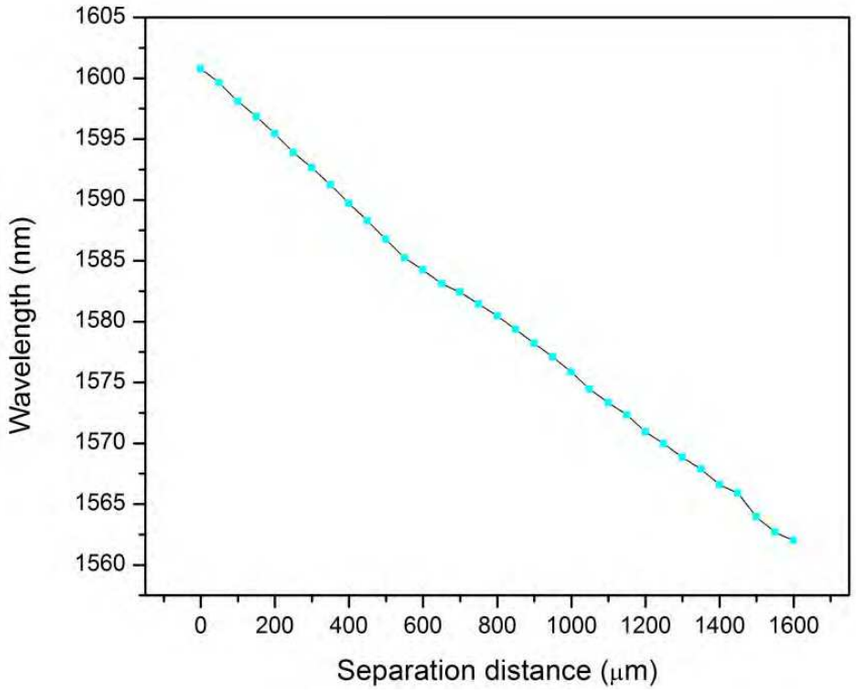

Fig. 19. Peak wavelength response of the MMI filter as a function of the separation distance between the fibers in the ferrule.

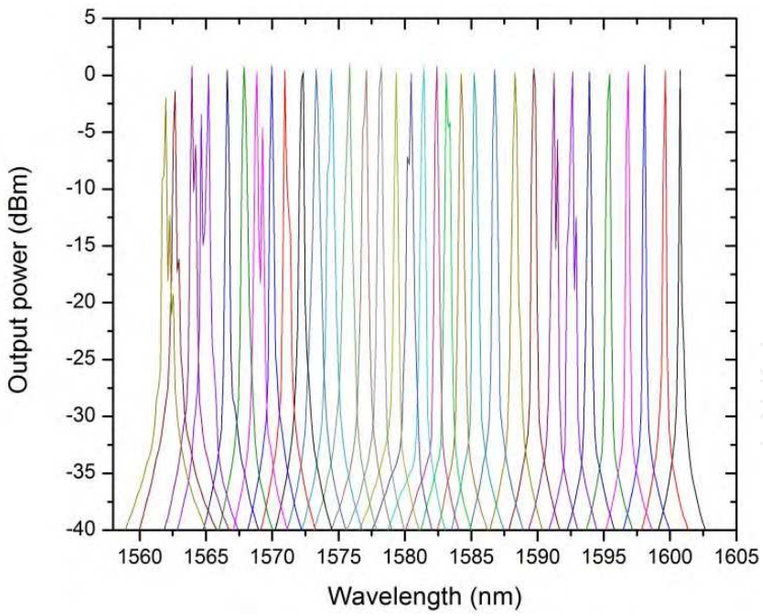

Fig. 20. Tuning range of 39nm, output power versus wavelength.

The second results obtained are shown in Fig. 21. Here, is shown the relation between the separation distance and the wavelength tuned. The wavelength tuning was achieved varying this separation in 1000 μm steps, within a total of 1.7 mm. the index matching fluid used was 1.45.

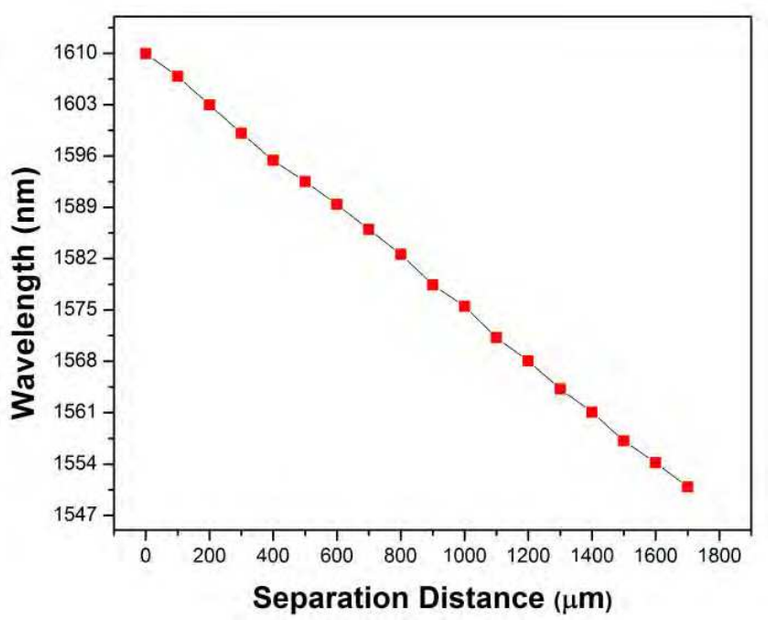

Fig. 21. Separation distance between fibers (single mode fiber and no-core) versus wavelength tuned.

As it can be seen, the total tunable range was limited by 60 nm. It was reported that a possible reason for this is the small mismatch between the diameter of the silica ferrule (127 μm) and that of the no-core fiber (125 μm) and also for the inner ferrule imperfections. So, every time the fibers were moving apart to each other, some kind of tilting between the facets end-fibers could deteriorate the coupling of the self-image to the output SMF. It is understood that a more uniform capillary with a diameter closer to the diameter of the MMF would increase the tuning range.

The complete tunable range is showed in Fig. 22. It is cleared that the peak wavelengths achieved in both tunable set ups differs. It is assumed that the difference on the index matching fluids affects directly in the optical spectrum wavelength as well as on the total tunable range because of the reduction of the loss inside of the liquid waveguide.

The total insertion loss was of 0.64 dB. The tunable range covered was of 60 nm which was from 1549 nm to 1609 nm. The measured laser linewidth was of 0.4 nm with a signal-to-noise ratio (SNR) of about 40 dB.

Since the wavelength peak response is a function of the MMF length, it could be possible to apply this system to other kind of rare-earth doped fiber laser in order to develop different wavelength ranges. Also, it is possible to apply this filter to high power application since the index matching liquids have boiling points of at least 100°C or implement it together with a master oscillator power amplifier (MOPA) configuration.

3.5 Numerical model for a high power erbium doped fiber laser

It was compute the evolution of a signal, pump, backward and forward ASE (Amplified Spontaneous emission) in a fiber laser in a model that takes into account the modal shape of the radiation fields, the spectral shape of cross sections and of forward and backward propagation ASE, pump power depletion, and saturations due to ASE and or signal. The

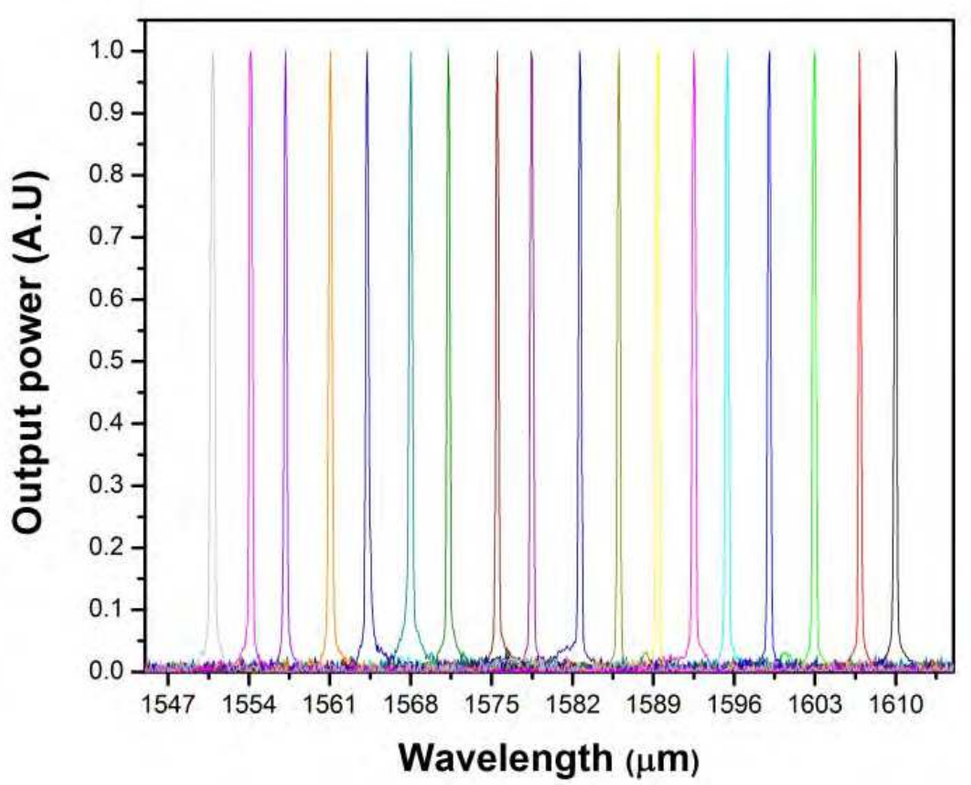

Fig. 22. Total tunable range of an EDFL based on the MMI effect.

model can be easily extended to different rare-earth fiber laser configuration subject to some constrains, since the physics remains the same in many cases. It is used the spectroscopy data of an erbium doped fiber from a published paper.

Rare-earth doped fibers offer many advantages for example: they are lightweight and flexible and can be coiled so that compactly packaged and robust devices can be carried out; they are well-controlled beam shape, owing to the confinement of light in the core of the fiber; the thermal management is simple thanks to the extended length, large surface area, and small transverse dimension of the fiber (Ueda et al., 2002). It can also find the rare-earth fibers good devices offering a high gain, and the use of a glass host leads to a wide bandwidth, which makes them suitable for amplifiers as well as for widely tunable lasers. Other attractive features of fibers lasers include narrow linewidth (with wavelength-selection), efficiency, stability, reliability, and temporal characteristics ranging from CW to femtosecond pulses. All these attractions make fiber lasers very useful in areas such as thermal printing, drilling, welding, cutting, material processing, nonlinear frequency conversion, remote pumping of EDFAs (Erbium Doped fiber Amplifiers), range finding, defense, aerospace, and medicine (Anthon et al., 2001; Jackson & Lauto, 2002). For those reasons, the rare-earth modeling is acquiring so much importance now in our days. This work is focus in the modeling of an erbium doped fibers seeded with a tunable fiber source based on the multimode interference effect.

3.5.1 The model

The equations do need to be solved numerically. Assuming again that the pump and the signal light are co-propagating, the numerical solution proceeds as follows: First, the (discretized) forward-travelling ASE spectrum and the pump and signal powers are propagated forward according to Eqs. (1) – (6) with $S\text{–}ASE = 0$ in Eq. (5).

$$\frac{dP(z,v)}{dz} = g_m(z,v)P(z,v) \tag{8}$$

$$g_m(v) = \int_0^\infty \Psi(r,v)\left[N_2(r,z)\left(\sigma_e(v) - \sigma_{ESA}(v)\right) - N_1(r,z)\sigma_a(v)\right]2\pi r dr \tag{9}$$

$$\gamma_e(z,v) = \sigma_e(v)\int \Psi(r,v)N_2(r,z)2\pi r dr \tag{10}$$

$$\frac{dS^+_{ASE}(z,v)}{d(\pm z)} = g_m(z,v)S^{\pm}_{ASE}(z,v) + 2hv\gamma_e(z,v) \tag{11}$$

$$\begin{aligned} R(r,z) &= \frac{P_p(z)\Psi(r,v_p)\sigma_a(v)}{hv_p} + \frac{P_p(z)\Psi(r,v_s)\sigma_a(v_s)}{hv_s} \\ &+ \int_0^\infty \Psi(r,v)\frac{S^+_{ASE}(z,v) + S^-_{ASE}(z,v)}{hv}\sigma_a(v)dv \end{aligned} \tag{12}$$

$$n_2 = \frac{R}{(R+W+A)} \tag{13}$$

The equations are integrated numerically, e.g. with a Runge-Kutta method. At the same time, the population inversion throughout the fiber is calculated. The resulting forward-travelling light powers are then used in Eq. (12) when Eq. (11) is integrated backward to yield the backward-travelling ASE spectrum. In the process, the population inversion is recalculated. Appropriate boundary conditions (determined by the endreflectors) are used to couple forward and backward-propagating light fields to each other. Then, Eq. (8) and Eq. (11) are integrated forward again, now including the $S\text{–}ASE(z,v)$ just found in Eq. (12). This process is repeated until convergence is reach. Other methods for solving Eqs. (8 and 12) exist, too. In the case of a laser, no signal is injected; instead, the lasing field builds up from spontaneous emission.

3.5.2 Results and discussion

Erbium-doped fiber laser is modeled as a three level system. It was pumped at 980nm, 10 W diode laser, to amplified light at 1567, that is, it was launched into it a seed signal at 1567nm in order to configure our experiment that would consists of a tunable erbium fiber laser feeding a double-clad erbium-doped fiber amplifier in a MOPA configuration and thus realizes a high power system together with our previous results of a MMI-effect-widely-tunable-fiber laser. Double-cladding-pumping has revolutionized fiber lasers over the last

decades. The perspective of that a single-mode diodes are limited in power to a few hundred miliwatts changed with the breakthrough idea, referred to as cladding-pumping (using double-clad fibers), patented by James Kafka at Spectra Physics (Kafka, 1989). A double-clad fiber, indeed, enables a good match with the output beam from broad-stripe diode. These are multi-mode devices that can generate much higher powers than single-mode ones. Thus, with cladding-pumping, a double-clad fiber laser can produce much higher output power, in a beam that nevertheless can be diffraction-limited. Cladding-pumped fiber lasers are currently considered for many applications, where high laser powers are required.

In Fig. 23 is plotted the values of the laser signal calculated in this fashion versus absorbed pump power. The system achieved a total output power of 2.64 Watts and with a threshold absorbed power of 0.3W. We obtained a slope efficiency of around 30%. The dopant concentration for our power regime was 300ppm wt% of erbium with a total fiber length of 10 m. Some parameters of the double cladding optical fiber were an inner cladding diameter of 30 μm, and out cladding diameter of 125 μm, a NA of 0.1 and a radius of 1.8×10^{-6} m. The model utilized can be easily extended and complete the all widely tunable seed signals (1549 nm to 1609 nm) for our double-clad erbium fiber laser simulated configuration, since the optics remains the same.

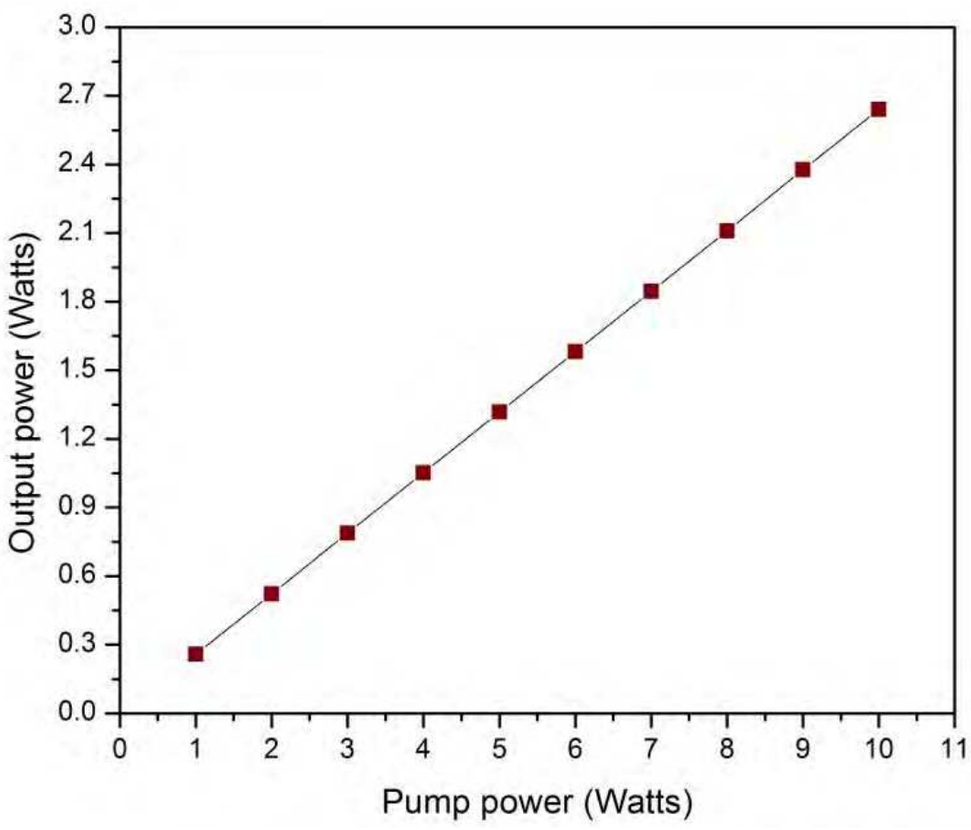

Fig. 23. Erbium results, output power versus pump power.

The results obtained in this part, were compared with other rare-earth doped-fiber simulations and it was realized that this work is highly reliable. It was utilized some spectroscopy data of important fiber fabrication companies as a base like the diameters of the fiber, indexes of refraction, pump wavelength, etc; that guarantee even more our work.

4. Conclusion

It has been demonstrated tunable rare-earth doped fiber lasers which based their tunable system in the multimode interference effect that occurs on the optical fibers. Different arrangements were used in order to apply this effect. Firstly, it was used a mirror and a facet fiber with a gold film as a reflecting device to induce the light back into the system and selecting the wavelength to tune by moving away the reflecting device from the final facet of the multimode fiber. The tunable range achieved with these optical lasers was as many as 8 nm and 12 nm respectively.

The following setup presented shows to be the most promising device, and it consisted in a device that works as a liquid waveguide inside of a ferrule filled it with an index matching fluid for a longer tunable range and for conserving the light propagation in one axis. The highlighted results showed a total tunable range of 60 nm which goes from 1549 nm to 1609 nm. The measured laser linewidth was of 0.4 nm with a signal-to-noise ratio (SNR) of about 40 dB.

In general this device is inexpensive and portable due to the simplicity of its elements. Also, these types of lasers are well applied to a variety of technologies such as optical communications and medicine.

It is also concluded by a simulation that a high power fiber laser that uses our optical filter as tunable device is possible to build up. An output power of 2.64 Watts was achieved within the optical range tuned of 60 nm. This device is very likely to scale even to higher powers along with different rare earth doped fiber lasers.

5. Acknowledgments

Special thanks to the National Mexican Council of Science and Technology (CONACYT), the Publical and Educational Secretary (SEP) and Physical and Mathematical Sciences Research Center (CICFIM) UANL-FCFM for all the support in the last years.

6. Nomenclature

SOA	Semiconductor Optical Amplifier
MMI	Multimode Interference
MOPA	Master Oscillator Power Amplifier
EDFL	Erbium Doped fiber Laser
DCEDF	Double Cladding Erbium Doped Fiber
MMF	Multimode Fiber

SMF Singlemode fiber

DCYDF Double Cladding Ytterbium Doped Fiber

AR Anti-Reflection Coating

YDFL Yterbium Doped Fiber Laser

DCYFL Double Cladding Yterbium Fiber Laser

SU-8 SU-8 photoresist

TEDFL Tunable Erbium Doped Fiber Laser

MMW Multimode Waveguide

FWHM Full Width at Half-Maximum

SNR Signal to Noise

ASE Amplified Spontaneous Emission

EDFA Erbium Doped Fiber Amplifier

NA Numerical Aperture

7. References

Chen, H., Babin, F., Leblanc, M., He, G. & Schinn G. W. (2003). 70-Nm Tunable Single-Longitudinal Mode Erbium-Doped Fiber Laser, *Proc. SPIE*, Vol. 4833, No. 956.

Xia, L., Shum, P., Wang, Y. X. & Cheng, T. H. (2006). Stable Triple-Wavelength Fiber Ring Laser With Ultranarrow Wavelength Spacing Using A Triple-Transmission-Band Fiber Bragg Grating Filter, *IEEE Photon. Technol. Lett.,* Vol. 18. No. 20, pp. 2162-2164.

Goh, C. S., Mokhtar, M.R., Butler, S.A., Set, S.Y., Kikuchi, K., & Ibsen, M. (2003). Wavelength Tuning Of Fiber Bragg Grating Over 90nm Using A Simple Tuning Package, *IEEE Photon. Technol. Lett*., Vol. 15, No. 4, pp. 557-559.

Mokhtar, M. R., Goh, C.S., Butler, S.A., Set, S.Y., Kikuchi, K., Richardson, D.J & Ibser, M. (2003). Fiber Bragg Grating Compression-Tuned Over 110nm, *Electron. Lett*., Vol. 39, No. 6, pp. 509-511.

Zhang, Z., Wu, J., Xiu, K., Hong, X. & J. Lin. (2009). Tunable Multiwavelength SOA Fiber Laser With Ultra-Narrow Wavelength Spacing Based On Nonlinear Polarization Rotation, *Opt. Express*, Vol. 17, No. 17, pp. 200-205.

Chawki, M. J., Valiente, I., Auffret, R. & Tholey, V. (1993). All Fibre, 1.5 Mu M Widely Tunable Single Frequency And Narrow Linewidth Semiconductor Ring Laser With Fibre Fabry Perot Filter, *Electron. Lett*., Vol. 42, No. 23, pp. 2034 – 2035.

Soldano, L., Veerman, F., Smit, M., Verbeek, B., Dubost, A. & Pennings, E. (1992). Planar Monomode Optical Couplers Based on Multimode Interference Effects, *Journal of Ligthwave Technology*, Vol. 10, No.12, pp. 1843-1850.

Mohammed, W., Mehta, A. & Johnson, E. (2004). Wavelength Tunable Fiber Lens Based on Multimode Interference, *Journal of Ligthwave Technology,* Vol. 22, No.2, pp. 469-477.

Soldano, L. & Pennings E. (1995). Optical Multi-Mode Interference Devices Based on Self-Imaging: Principles and Applications, *Journal of Ligthwave Technology*, Vol. 13, No.4, pp. 615-627.

Li, B., Chua, S., Leitz, C. & Fitzgerald, E. (2002). 1x2 Optical Waveguide Filters Based on Multimode Interference for 1.3- and 1.55-μm Operation, *Optical Engineering,* Vol. 41, pp. 723.

Selvas, R., Torres-Gomez, I., Martinez-Rios, A., Alvarez-Chavez, J.; May-Arrioja, D., LiKamWa, P., Mehta, A. & Johnson, E. (2005). Wavelength Tuning of Fiber Lasers Using Multimode Interference Effects, *Optics Express,* Vol. 13, No. 23, pp. 9439-9445.

Anzueto-Sánchez, G., Martínez-Ríos, A., May-Arrioja, D., Torres-Gómez, I., Selvas-Aguilar, R. & Alvárez-Chávez, J. (2006). Enhanced Tuning Mechanism in Fiber Laser Based on Multimode Interference Effects, *Electronic Letters*, Vol. 42, No. 23, pp. 1337-1338.

Mehta, A., Mohammed, W. & Johnson, E. (2003). Multimode Interference-Based Fiber-Optic Displacement Sensor, *Photonic Technology Letters*, Vol. 15, No. 8, pp. 1129-1131.

Poustie, J., Finlayson, N. & P. Harper. (1994). Multiwavelength Fiber Laser Using A Spatial Mode Beating Filter, *Opt. Lett.*, Vol. 19, pp. 716-718.

Wang, Q. & Farrell, G. (2006). All-Fiber Multimode-Interference-Based Refractometer Sensor: Proposal And Design, *Opt. Lett*. Vol. 31, pp. 317-319.

Li, Q., Lin, C., Tseng, P. & Lee, H. P. (2005). Demonstration Of High Extinction Ratio Modal Interference In A Two-Mode Fiber And Its Application For All-Fiber Comb Filter And High-Temprerature Sensor, *Opt. commun.*, Vol. 250, pp. 280-285.

Martinez-Rios, A., Starodumov, A., Po, H., Wang, Y. & Demidov, A. (2003). Efficient Operation of Double-Clad Yb-Doped Fiber Lasers with a Novel Circular Cladding Geometry, *Optics Letters*, Vol. 28, pp. 1642-1644.

Raymond, C. & Johnson, E. (2004). Micro-Photonic Systems Utilizing SU-8. *Proceedings of SPIE 2004 MOEMS and Miniaturized Systems IV*, pp. 64–69.

Antonio-Lopez J., Castillo-Guzman A., May-Arrioja D., Selvas-Aguilar R. & LiKamWa P. (2010). Tunable Multimode-Interference Bandpass Fiber Filter, *Opt. Lett*. Vol. 35, pp. 324-326.

Mohammed W., Smith P. & Gu X. (2006). All-Fiber Multimode Interference Bandpass Filter, *Opt. Lett.*, Vol. 31, pp. 2547-2549.

Castillo-Guzman, A., Antonio-Lopez, J., Selvas-Aguilar, R., May-Arrioja, D., Estudillo-Ayala, J. & LiKamWa P. (2010). Widely Tunable Erbium-Doped Fiber Laser Based On Multimode Interference Effect, *Opt. Express,* Vol. 18, pp. 591-597.

Ueda, K.I., Sekiguchi, H. & Kan H. (2002). 1 Kw Cw Output From Fiber Embedded Lasers, *in Proc. Conference on Lasers and Electro-Optics*, Vol. CPDC4.

Anthon, D., Fisher, J., Keur, M., Sweeney, K., Ott, D., Matton, P. & Emslie, C. (2001). High Power Optical Amplifiers For CATV Applications, *Optical Fiber Communication Conference*, Vol. 2.

Jackson, S. D & Lauto, A. (2002). Diode-Pumped Fiber Lasers: A New Clinical Tool, *Lasers in surgery and Medicine*, Vol. 30, pp. 184-190.

Kafka J. (1989). Laser Diode Pumped Fiber Laser With Pump Cavity. US Patent 4, 829.

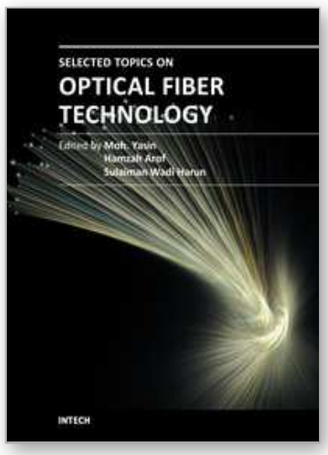

Selected Topics on Optical Fiber Technology

Edited by Dr Moh. Yasin

ISBN 978-953-51-0091-1

Hard cover, 668 pages

Publisher InTech

Published online 22, February, 2012

Published in print edition February, 2012

This book presents a comprehensive account of the recent advances and research in optical fiber technology. It covers a broad spectrum of topics in special areas of optical fiber technology. The book highlights the development of fiber lasers, optical fiber applications in medical, imaging, spectroscopy and measurement, new optical fibers and sensors. This is an essential reference for researchers working in optical fiber researches and for industrial users who need to be aware of current developments in fiber lasers, sensors and other optical fiber applications.

How to reference

In order to correctly reference this scholarly work, feel free to copy and paste the following:

Arturo A. Castillo-Guzman and Romeo Selvas-Aguilar (2012). Tunable Rare-Earth Doped Fiber Laser, Selected Topics on Optical Fiber Technology, Dr Moh. Yasin (Ed.), ISBN: 978-953-51-0091-1, InTech, Available from: http://www.intechopen.com/books/selected-topics-on-optical-fiber-technology/tunable-rare-earth-doped-fiber-lasers-

INTECH
open science | open minds

InTech Europe
University Campus STeP Ri
Slavka Krautzeka 83/A
51000 Rijeka, Croatia
Phone: +385 (51) 770 447
Fax: +385 (51) 686 166
www.intechopen.com

InTech China
Unit 405, Office Block, Hotel Equatorial Shanghai
No.65, Yan An Road (West), Shanghai, 200040, China
中国上海市延安西路65号上海国际贵都大饭店办公楼405单元
Phone: +86-21-62489820
Fax: +86-21-62489821

IntechOpen